

# The Apaf-1-binding protein Aven is cleaved by Cathepsin D to unleash its anti-apoptotic potential

IM Melzer<sup>1,7</sup>, SBM Fernández<sup>1,7,8</sup>, S Bösser<sup>1</sup>, K Lohrig<sup>2</sup>, U Lewandrowski<sup>2</sup>, D Wolters<sup>3</sup>, S Kehrlöesser<sup>1,9</sup>, M-L Brezniceanu<sup>1,10</sup>, AC Theos<sup>4</sup>, PM Irusta<sup>4</sup>, F Impens<sup>5,6</sup>, K Gevaert<sup>5,6</sup> and M Zörnig<sup>\*,1</sup>

The anti-apoptotic molecule Aven was originally identified in a yeast two-hybrid screen for Bcl-x<sub>L</sub>-interacting proteins and has also been found to bind Apaf-1, thereby interfering with Apaf-1 self-association during apoptosome assembly. Aven is expressed in a wide variety of adult tissues and cell lines, and there is increasing evidence that its overexpression correlates with tumorigenesis, particularly in acute leukemias. The mechanism by which the anti-apoptotic activity of Aven is regulated remains poorly understood. Here we shed light on this issue by demonstrating that proteolytic removal of an inhibitory N-terminal Aven domain is necessary to activate the anti-apoptotic potential of the molecule. Furthermore, we identify Cathepsin D (CathD) as the protease responsible for Aven cleavage. On the basis of our results, we propose a model of Aven activation by which its N-terminal inhibitory domain is removed by CathD-mediated proteolysis, thereby unleashing its cytoprotective function.

*Cell Death and Differentiation* (2012) 19, 1435–1445; doi:10.1038/cdd.2012.17; published online 2 March 2012

Two important apoptosis signal-transduction pathways have been delineated in recent years. Whereas the extrinsic pathway is exclusively triggered by activation of a specific subclass of the TNF receptor superfamily, the so-called death receptors, an important and integral part of the intrinsic mitochondrial apoptosis pathway involves the release of several pro-apoptotic molecules, including Cyt *c*, from the mitochondria into the cytosol.<sup>1,2</sup> Subsequent Cyt *c*/dATP-dependent formation of the Caspase-9-activating apoptosome protein complex requires oligomerization of the adaptor protein Apaf-1 for Caspase-9 recruitment and activation.<sup>3,4</sup>

To prevent the severe patho-physiological consequences of the deregulation of mitochondrial apoptosis, apoptosome activity is tightly regulated. Defects in the mitochondrial apoptosis pathway have been linked to various pathologies such as heart attack, stroke, liver failure, autoimmune diseases and cancer (for a review see D'Amelio *et al.*,<sup>5</sup> Hajra and Liu,<sup>6</sup> and Ledgerwood and Morison<sup>7</sup>). Failure to form a functional apoptosome complex and initiate the caspase

cascade by activating Caspase-9 contributes to tumor development, the progression of several malignancies and also has a significant role in the development of cancer therapy resistance. Therefore, tight regulation of apoptosome activation is critical for normal homeostasis.

Several intracellular apoptosis inhibitors have been reported to prevent Apaf-1 oligomerization, for example, prothymosin alpha (ProT<sup>8,9</sup>) and the heat shock proteins 70 and 90.<sup>10–12</sup> Another anti-apoptotic molecule with apoptosome-regulating activity is Aven. Although initially identified in a yeast two-hybrid screen for Bcl-x<sub>L</sub>-interacting proteins,<sup>13</sup> Aven has also been found to bind to Apaf-1, thereby interfering with Apaf-1 self-association during apoptosome assembly. Whether the interaction of Aven with Bcl-x<sub>L</sub> contributes to its anti-apoptotic activity<sup>14</sup> or it is in fact dispensable<sup>13</sup> remains an open question.

Interestingly, two recent publications have reported increased Aven protein levels in acute leukemias. Aven overexpression was found to be associated with poor

<sup>1</sup>Chemotherapeutisches Forschungsinstitut Georg-Speyer-Haus, Paul-Ehrlich-Strasse 42-44, Frankfurt D-60596, Germany; <sup>2</sup>Leibniz-Institut für Analytische Wissenschaften, ISAS e.V., Bunsen-Kirchhoff-Str. 11, Dortmund D-44139, Germany; <sup>3</sup>Biomolecular Mass Spectrometry, Analytical Chemistry Department, Ruhr-University Bochum, Universitätsstrasse 150, Bochum D-44801, Germany; <sup>4</sup>Department of Human Science, Georgetown University Medical Center, Georgetown University, Washington, DC 20057, USA; <sup>5</sup>Department of Medical Protein Research, VIB, Ghent, Belgium and <sup>6</sup>Department of Biochemistry, Ghent University, Ghent, Belgium

\*Corresponding author: M Zörnig, Chemotherapeutisches Forschungsinstitut, Georg-Speyer-Haus, Paul-Ehrlich-Strasse 42-44, Frankfurt D-60596, Germany.

Tel: +49 69 63395115; Fax: +49 69 63395297; E-mail: zoernig@em.uni-frankfurt.de

<sup>7</sup>These authors contributed equally to this work.

<sup>8</sup>Current address: Department of Immunology and Oncology, National Center for Biotechnology (CNB), CSIC, Madrid 28049, Spain.

<sup>9</sup>Current address: Institute of Biophysical Chemistry and Center for Biomolecular Magnetic Resonance and Cluster of Excellence Macromolecular Complexes (CEF), Goethe University, Frankfurt D-60438, Germany.

<sup>10</sup>Current address: Research Centre, Centre hospitalier de l'Université de Montréal (CHUM)-Hôtel-Dieu, Montréal, Québec, Canada.

**Keywords:** Aven; Cathepsin D; proteolysis; mitochondrial apoptosis pathway

**Abbreviations:** Ac-DEVD-AFC, N-acetyl-Asp-Glu-Val-Asp-7-amino-4-trifluoromethylcoumarin; Apaf-1, apoptotic protease activating factor 1; ATM, ataxia telangiectasia mutated; Bcl-x<sub>L</sub>, B cell lymphoma extra large; Bcl-2, B-cell lymphoma 2; Bid, BH3 interacting domain death agonist; CathD, Cathepsin D; CED-4, cell death abnormality 4; Cyt *c*, cytochrome *c*; dATP, desoxy-adenosine-triphosphate; DMEM, Dulbecco's modified Eagle's medium; DMSO, dimethyl sulfoxide; DTT, dithiothreitol; EDTA, ethylenediaminetetraacetic acid; E64, N-[N-(L-3-*trans*-carboxyirane-2-carbonyl)-L-leucyl]-L-arginine; FasL, Fas ligand; FBS, fetal bovine serum; GFP, green fluorescent protein; IP, immunoprecipitation; LAV, large intracellular acidic vesicles; MES, 2-(*N*-morpholino)ethanesulfonic acid; NaCl, sodium chloride; NHS AcD<sub>3</sub>-acetate, N-hydroxysuccinimide trideutero-acetate; PEI, polyethylenimine; pAPMSF, p-amidino-phenylmethylsulfonylfluoride; ProT, prothymosin alpha; RPMI, 1640 Roswell Park Memorial Institute; TNF, tumor necrosis factor; z-VAD, carbobenzoxy-valyl-alanyl-aspartyl-[O-methyl]-luoromethylketone

Received 24.2.11; revised 25.1.12; accepted 30.1.12; Edited by JM Hardwick; published online 02.3.12

prognosis in childhood acute lymphoblastic leukemia, and it has been suggested as a novel prognostic indicator in these malignancies.<sup>15,16</sup> These correlative studies suggest a potential oncogenic role for the anti-apoptotic protein Aven in acute leukemias.

Since the original report published by Chau *et al.*,<sup>13</sup> no additional information regarding the molecular mechanism of apoptosis inhibition by Aven has been reported. In particular, the mechanism by which the activity of this ubiquitous apoptosis inhibitor is controlled remains unclear, as Aven is expressed in a wide variety of adult tissues and cell lines. In this study, we demonstrate that for the activation of its anti-apoptotic potential the inhibitory Aven N-terminus must be cleaved by Cathepsin D (CathD). Therefore, it is the

proteolytic processing by CathD rather than the absolute expression levels that determine the anti-apoptotic potential of Aven within the cell, a finding that may have implications for therapeutic targeting of Aven activity during tumorigenesis.

## Results

**Deletion of the N-terminus is required for efficient inhibition of mitochondrial apoptosis by the anti-apoptotic protein Aven.** We performed a functional yeast survival screen with a human breast carcinoma-derived cDNA library in order to identify novel anti-apoptotic proteins involved in tumorigenesis.<sup>17,18</sup> Among others, we isolated a cDNA clone coding for an N-terminal deletion mutant of the anti-apoptotic Aven protein. This clone, which efficiently suppressed yeast cell death induced by the pro-apoptotic *C. elegans* protein CED-4 (see Supplementary Figure 1), lacks the coding sequence for the N-terminal 179 aa (amino acid) of the protein ( $\Delta N$ -Aven 180–362). The construct most likely represents an artifact generated during library production rather than a naturally occurring transcript of a truncated Aven isoform, as no splicing sites are predicted at or near the gene region where the 5' end of  $\Delta N$ -Aven 180–362 is located.

To analyze the anti-apoptotic potential of  $\Delta N$ -Aven 180–362 in a mammalian cell system, human colon carcinoma type II<sup>19</sup> RKO cells were transfected with plasmids coding for either the full-length Aven or  $\Delta N$ -Aven 180–362 and subsequently treated with the death stimulus Fas Ligand (FasL). Surprisingly, transfection of full-length Aven did not protect against FasL-induced cell death, whereas  $\Delta N$ -Aven 180–362 significantly inhibited apoptosis (Figure 1a). We also investigated the potential of Aven and  $\Delta N$ -Aven 180–362 to inhibit

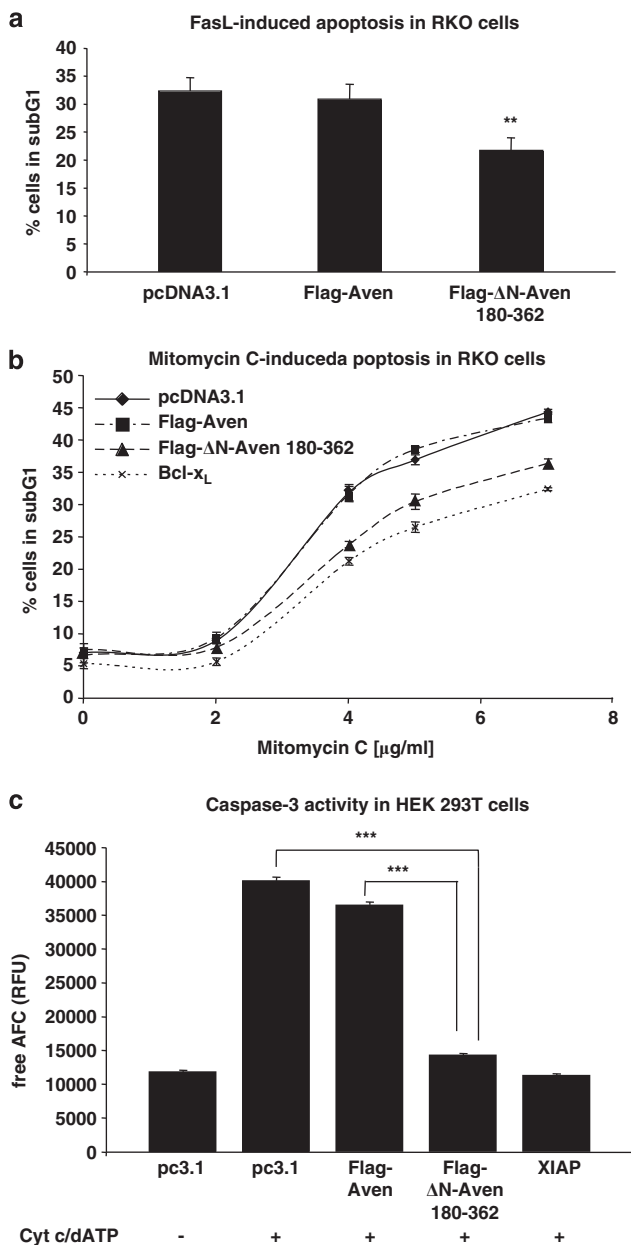


**Figure 1**  $\Delta N$ -Aven 180–362 suppresses mitochondrial apoptosis while full-length Aven fails to prevent cell death. (a) RKO cells transiently transfected with pcDNA3.1 (empty vector), full-length Flag-Aven or Flag- $\Delta N$ -Aven 180–362 were treated for 16 h with FasL (20 ng/ml). Levels of apoptosis in treated cells were quantified as the percentage of cells in the subG1 phase in three independent flow cytometry experiments. The Student's *t*-test was used to assess the statistical significance of the Flag-Aven and Flag- $\Delta N$ -Aven results ( $P \leq 0.01$ ). (b) RKO cells were transiently transfected with empty vector pcDNA3.1 (negative control), full-length Flag-Aven, Flag- $\Delta N$ -Aven 180–362 or Bcl-x<sub>L</sub> (positive control). Cells were then treated with various concentrations of mitomycin C. After 16 h, apoptosis was quantified by flow cytometry. The mean values of three independent experiments (each in duplicate) are shown. A one-way ANOVA test was performed with a LSD/Bonferroni *post-hoc* analysis to test for significant differences between the two constructs (at varying concentrations of mitomycin C). The variations between the Flag-Aven, Flag- $\Delta N$ -Aven 180–362, and Bcl-x<sub>L</sub> results are highly significant at 4.5 and 7  $\mu$ g/ml mitomycin C ( $P \leq 0.001$ ). (c) Caspase-3 activity was measured in extracts derived from the HEK 293T cells previously transfected with empty vector pcDNA3.1 (pc3.1), full-length Flag-Aven, Flag- $\Delta N$ -Aven 180–362, or XIAP (Caspase-3 inhibitor). Cell lysates were incubated in the presence (+) or absence (-) of Cyt c and dATP to induce apoptosome formation. Caspase-3 activity was then quantified fluorometrically upon cleavage of the added DEVD-AFC substrate. The mean values of eight independent experiments (each performed in triplicate) are shown. The mean Caspase-3 activity in lysates containing Flag- $\Delta N$ -Aven 180–362 was significantly decreased compared to lysates of cells transfected with pcDNA3.1 or Flag-Aven ( $P \leq 0.001$ , One-way ANOVA with Games–Howell *post-hoc* analysis). The bars in a–c represent standard errors with \*\* and \*\*\* indicating  $P \leq 0.01$  and  $P \leq 0.001$ , respectively

cell death induced by mitomycin C, a potent DNA crosslinker used in cancer treatment to induce mitochondrial apoptosis.<sup>20,21</sup> Figure 1b shows that  $\Delta$ N-Aven 180–362 and the *bona fide* apoptosis inhibitor Bcl-x<sub>L</sub> both significantly inhibited apoptosis caused by mitomycin C at different concentrations, whereas expression of full-length Aven did not confer protection under this experimental paradigm.

Failure of full-length Aven to inhibit apoptosis was confirmed by measuring Caspase-3 activity in the cell lysates prepared from transfected human embryonic kidney (HEK) 293T cells that were subsequently activated for apoptosome formation by addition of exogenous Cyt *c* and dATP. Using this *in vitro* system, we found that upon activation, lysates from cells transfected with Flag-tagged full-length Aven displayed levels of Caspase-3 activity that were similar to those of the control lysates (i.e., cells that had been transfected with empty vector; see Figure 1c). In contrast, lysates from cells overexpressing Flag-tagged  $\Delta$ N-Aven 180–362 showed significantly lower levels of Caspase-3 activity when compared with control lysates, displaying values comparable to those obtained with lysates from cells overexpressing the caspase inhibitor XIAP.

**The inhibitory Aven N-terminus is removed by CathD-dependent cleavage.** Our results suggest that the Aven N-terminus yields an inhibitory influence, which requires neutralization before the protein is capable of exerting its anti-apoptotic activity. As  $\Delta$ N-Aven 180–362 most likely represents a cloning artifact generated during cDNA library production, we analyzed different cell lines in search for naturally occurring smaller Aven isoforms. Full-length Aven was also overexpressed in the mammary adenocarcinoma cell line MCF-7 and in HEK 293T cells, and protein expression was subsequently analyzed via immunoblot assay using an antibody that specifically recognizes the C-terminus of Aven (Aven CT). Expression analysis revealed that in addition to the full-length Aven protein, a further immunoreactive band of ~30 kDa was present in cell lysates, which is similar in size to the artificial  $\Delta$ N-Aven 180–362 (see Figure 2a). Interestingly, this truncated form of Aven lacking the N-terminus occasionally appears as a doublet in MCF-7 cells (between 26 and 30 kDa), whereas only one band is detected in 293T cells (bands labeled with arrowheads). We confirmed the specificity of these bands in MCF-7 cells by knocking down Aven expression. Although both the endogenous full-length Aven protein and the 30-kDa C-terminal Aven fragment were detected in cells transduced with a lentiviral control vector, they were either significantly reduced or absent in cells stably transduced with Aven shRNA (Figure 2b).

The presence of a truncated form of Aven in two independent cell lines suggests that Aven could be subjected to intracellular processing. To test whether a protease was responsible for generating the 30-kDa Aven fragment, we treated MCF-7 cells with various protease inhibitors (Figure 2c). While incubation with the cysteine protease inhibitor E64<sup>22</sup> and the caspase inhibitor z-VAD<sup>23</sup> showed no influence on Aven processing, the serine protease inhibitor aprotinin<sup>24</sup> and the serine and cysteine protease inhibitor pAPMSF<sup>25</sup> both significantly hampered the production of the

30-kDa C-terminal Aven form. Interestingly, treating cells with pepstatin A, an inhibitor of aspartic proteases and specifically of CathD,<sup>26</sup> entirely abolished Aven cleavage, thereby leading to a complete absence of the 30-kDa Aven fragment (Figure 2c, upper panel). A dose–response experiment using various concentrations of pepstatin A confirmed that 10  $\mu$ M of the inhibitor is sufficient to substantially suppress Aven proteolysis (Figure 2c, lower panel).

CathD is a prominent member of the subfamily of lysosomal aspartic proteases, and its enzymatic function is not restricted solely to the acidic milieu of lysosomes (for a review see Liaudet-Coopman *et al.*<sup>27</sup> and Masson *et al.*<sup>28</sup>). CathD has been implicated in positive and negative regulation of apoptosis, and its overexpression has been reported to promote tumorigenesis and metastasis of breast cancer (for a review see Masson *et al.*<sup>28</sup> and Garcia *et al.*<sup>29</sup>). Using lentiviral shRNA constructs we investigated whether CathD was required for Aven processing. Remarkably, stable knockdown of *CathD* in MCF-7 cells by the *CathD* shRNA CD1 resulted in a complete absence of the endogenous 30-kDa C-terminal  $\Delta$ N-Aven fragment (see Figure 2d, middle lane). Similarly, partial knockdown of *CathD* via the shRNA CD2 led to a significant reduction of the 30-kDa  $\Delta$ N-Aven fragment (Figure 2d, right lane). These results indicate that CathD is either directly or indirectly involved in the removal of the inhibitory Aven N-terminus.

To further examine the nature of the 30-kDa Aven fragment resulting from the cleavage by CathD and to confirm whether we could also detect a corresponding N-terminal peptide, we performed immunoblot analysis of lysates prepared from 293T cells, which had been transfected with full-length Aven,  $\Delta$ N-Aven (180–362), Aven 1–180, Aven 1–140 or Aven 140–362. The membranes were incubated with anti-Aven A antiserum recognizing the Aven N-terminus<sup>13</sup> and the Aven CT antiserum binding to the Aven C-terminus. For a better overview, the binding sites of these antisera within the Aven protein are indicated in the schematic diagram presented in Figure 3c. Using the N-terminal anti-Aven A antiserum, we detected full-length Aven protein and (in the same lane) a band running at approximately 27 kDa representing the N-terminal Aven fragment generated by CathD cleavage (Figure 2e, left panel, second lane, labeled with an arrowhead). The corresponding C-terminal Aven fragment resulting from CathD proteolysis was detected by the anti-Aven CT antiserum (Figure 2e, right panel, second lane, lower band labeled with arrowhead). In the anti-Aven A immunoblot, the polypeptide Aven 1–180 is running at a similar size compared with the 27-kDa N-terminal Aven cleavage product in full-length Aven-transfected cell lysates, thereby indicating that the main CathD cleavage site within the Aven molecule is in close proximity to aa position 180 (on the basis of our mass spectrometry results presented in Figure 3B, the cleavage site is located between aa 196 and 197, see below). This conclusion is supported by the observation that the C-terminal Aven fragment produced by CathD cleavage and recognized by the anti-Aven CT antiserum is running at a similar size compared with  $\Delta$ N-Aven 180–362 (Figure 2e, right panel, second and third lane). Interestingly, a weaker and larger fragment was detected with the anti-Aven CT antiserum in full-length Aven-transfected cell lysates (second lane, upper band

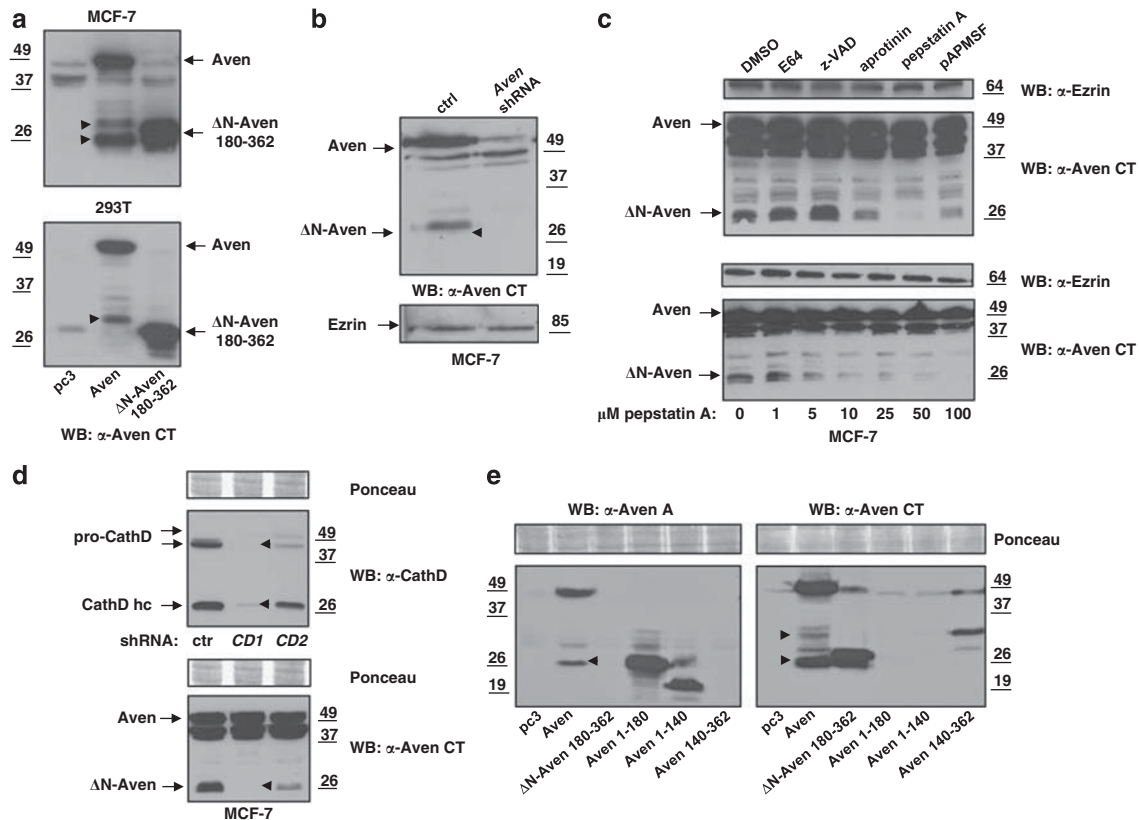


**Figure 2** CathD removes the inhibitory Aven N-terminus. (a) MCF-7 and HEK 293T cells were transfected with *pcDNA3.1* (pc3.1), *pcDNA3.1* full-length Flag-Aven (Aven) or *pcDNA3.1*  $\Delta$ N-Aven 180–362, and western blot analysis was performed using an antibody directed against the Aven CT (anti-Aven CT, *ProSci*). In both cell lines transfected with full-length Aven, a smaller  $\Delta$ N-Aven fragment of approximately 30 kDa was detected (labeled with arrowheads). In MCF-7 cells, this band appears as a doublet. (b) MCF-7 cells were transfected with either *pLKO.1 puro* containing a non-target control shRNA (control; ctrl) or *pLKO.1 puro Aven shRNA* (Aven shRNA). After puromycin selection of a stable cell pool, cell lysates were prepared for an immunoblot assay with the anti-Aven CT antibody. An endogenous 30-kDa  $\Delta$ N-Aven fragment (visible in the control shRNA-transduced cells, labeled with an arrowhead) disappeared together with the full-length protein upon Aven knockdown. Equal protein loading was demonstrated by incubation of the membrane with anti-Ezrin antibody. (c) Pepstatin A treatment prevents formation of  $\Delta$ N-Aven. Upper panel: MCF-7 cells were treated with the following protease inhibitors for 24 h: E64 (50  $\mu$ M; inhibits cysteine proteases), z-VAD-fmk (20  $\mu$ M; caspases), aprotinin (20  $\mu$ g/ml; serine proteases), pepstatin A (50  $\mu$ M; aspartic proteases), pAPMSF (100  $\mu$ M; serine and cysteine proteases) and DMSO (20  $\mu$ l; solvent control). The cells were harvested for preparation of protein lysates, and endogenous full-length and  $\Delta$ N-Aven were detected by immunoblotting with an anti-Aven CT antibody. Lower panel: MCF-7 cells were treated for 24 h with various pepstatin A concentrations. (d) CathD knockdown abrogates formation of  $\Delta$ N-Aven. MCF-7 cells were transfected with either non-target control shRNA (control; ctrl) or one of two different *CathD*-specific shRNAs (CD1, CD2). After puromycin selection of stable cell pools, immunoblot analysis was performed with anti-Cathepsin D and anti-Aven CT antibodies. Equal protein loading was demonstrated using Ponceau S staining of the membranes. The arrowheads indicate complete lack of CathD expression and the absence of endogenous  $\Delta$ N-Aven in CD1-transduced cells. CathD hc: CathD heavy chain. (e) HEK 293T cells were transfected with *pcDNA3.1* (pc3.1), *pcDNA3.1* full-length Flag-Aven (Aven), *pcDNA3.1*  $\Delta$ N-Aven 180–362, *pcDNA3.1* Aven 1–180, *pcDNA3.1* Aven 140–362. Western blot analysis was performed using the Aven A antiserum from Chau *et al.*,<sup>13</sup> which recognizes aa 98–112, thereby detecting N-terminal Aven fragments, and an antibody directed against the Aven CT (anti-Aven CT, *ProSci*). Arrowheads indicate the N-terminal Aven fragment (anti-aven A, left panel) and the C-terminal  $\Delta$ N-Aven fragment (anti-Aven CT, right panel) generated by CathD cleavage of overexpressed full length Aven. As expected from the binding sites, the anti-Aven A antiserum was not able to detect  $\Delta$ N-Aven 180–362 and Aven 140–362 (left panel), whereas the anti-Aven CT antiserum did not recognize Aven 1–180 or Aven 1–140 (right panel)

labeled with an arrowhead), which corresponds in size to Aven 140–362 (Figure 2e, right panel, sixth lane). According to our mass spectrometry results (Figure 3b), this fragment may result from Aven protein cleavage by CathD at aa position 144/145.

We performed a cleavage assay using recombinant human CathD and His-tagged full-length Aven protein purified from HEK 293T cells to investigate whether Aven represents a direct CathD target. At pH 6.5, CathD treatment generated a 30-kDa C-terminal fragment from full-length Aven, which could be detected by western blot analysis in a time-dependent manner (Figure 3a). Addition of the CathD inhibitor pepstatin A prevented the formation of the truncated Aven

form, and incubation for two hours without recombinant CathD failed to result in cleavage of the full-length Aven protein (data not shown). Thus, CathD can directly cleave Aven, thereby resulting in the generation of a 30-kDa  $\Delta$ N-Aven fragment.

To define the exact CathD cleavage sites, we analyzed a CathD digest of purified His-tagged Aven protein, both in the presence and absence of pepstatin A, using a mass spectrometry-based positional proteomics approach. The cleavage of proteins by proteases generates new alpha-N-termini (on the C-terminal fragments that are created), and these new primary amino groups can be marked with small tags that are easily identified following mass spectrometry and a database search. Here, the primary amino groups introduced

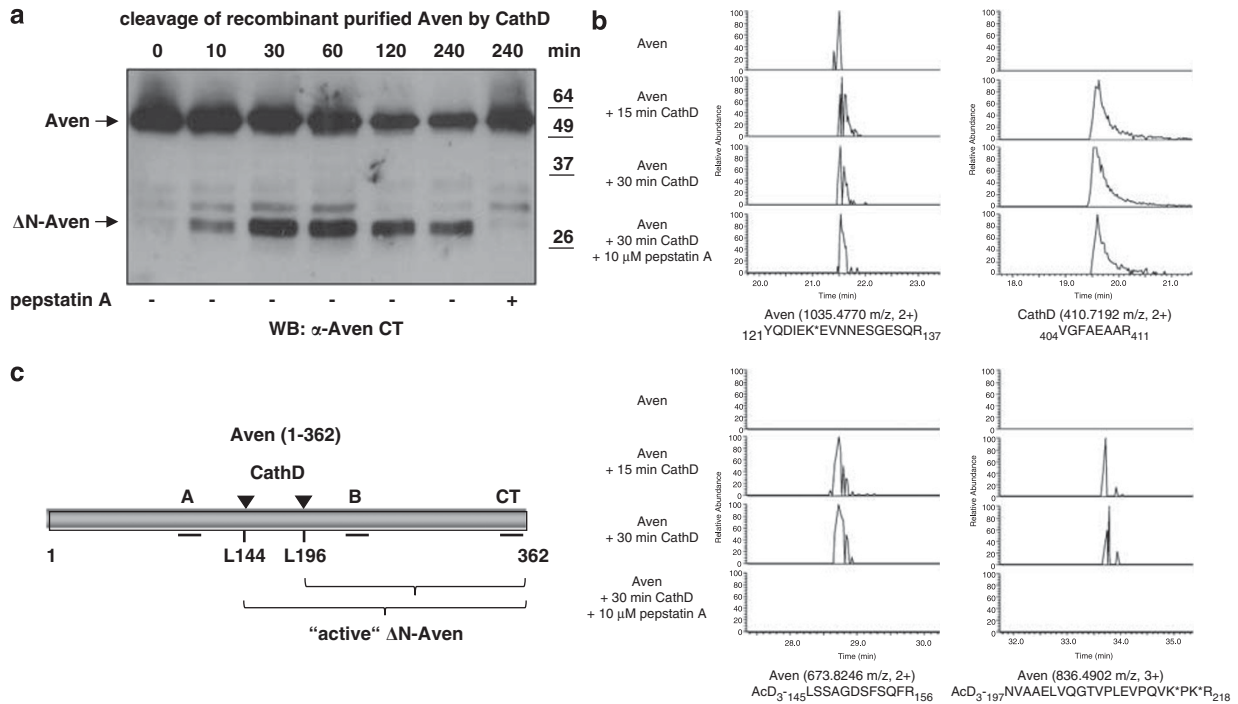


**Figure 3** Identification of CathD cleavage sites in the Aven protein by mass spectrometry. (a) Full-length Aven purified from HEK 293T cells was incubated with recombinant human CathD at pH 6.5. Time-dependent direct cleavage of Aven by CathD was evaluated by western blot analysis using the anti-Aven CT antiserum. Incubation for two hours without recombinant CathD failed to result in cleavage of the full-length Aven protein (data not shown). (b) Purified Aven protein was incubated with recombinant CathD, and newly formed alpha-N-terminal amines (and epsilon amines of lysine side-chains) were modified using trideutero-acetylation. Following trypsin digestion, LC-MS/MS analysis and peptide identification, peptides with trideutero-acetylated alpha-N-termini were considered as proteolysis-reporter peptides indicative of CathD processing. Extracted ion chromatograms (XIC) are shown for selected Aven and CathD peptides. Internal tryptic peptides with primary alpha-N-termini demonstrated the presence of both proteins in each sample (two upper panels). Two peptides with trideutero-acetylated N-termini reported protease cleavage at two positions in the Aven sequence when CathD was present without pepstatin A (two lower panels). Trideutero-acetylated lysine side-chains are indicated with an asterisk (\*), and maximum Mascot score/threshold values were 139/38 (YQDIEK\*EVNNEGESQR), 66/40 (VGFAEAAR), 62/39 (AcD<sub>3</sub>-LSSAGDSFSQFR) and 80/34 (AcD<sub>3</sub>-NVAELVQGTVPLEVPQVK\*PK\*R). (c) A schematic diagram of the N-terminally Flag-tagged human Aven protein (aa 1–362). The binding sites for antisera used in this study (Aven CT, Aven A and Aven B) are indicated by black lines. The CathD cleavage sites (L144 and L196) that were identified by mass spectrometry analysis are labeled with arrowheads. Active ΔN-Aven represents the C-terminal fragment(s) produced by CathD cleavage, which displays anti-apoptotic activity

by the CathD cleavage of Aven were chemically labeled with a trideutero-acetyl group (note that the epsilon-amines on lysines are also modified by the same group). Subsequent further processing by trypsin (performed to generate peptides that are identifiable by MS/MS) yields two classes of peptides: N-trideutero-acetylated protein N-terminal peptides and internal peptides holding a primary, non-trideutero-acetylated amino group. The former directly suggests processing by CathD, whereas the latter simply indicates the presence of Aven protein in the sample. According to this analysis, in the absence of pepstatin A, Aven was cleaved by CathD at sites located between aa 144/145 and between aa 196/197 (see Figure 3b). Both cleavage sites (together with the binding sites of the antisera used in this study) are indicated in the schematic diagram of Aven protein shown in Figure 3c.

Taken together, these data strongly suggest that the cleaved Aven molecules observed in cells are direct products of CathD-mediated cleavage.

**Aven and CathD partly co-localize in endosomal particles.** Proteolytic removal of the inhibitory Aven N-terminus by CathD can only occur with endogenous proteins *in vivo* if both proteins co-localize within the cell

during the processing of Aven. To investigate whether endogenous Aven and CathD co-localize intracellularly we performed immunofluorescence studies using MCF-7 cells. As expected, CathD staining resulted in a characteristic punctuate pattern typical of lysosomal/endosomal localization (Figure 4, upper panels). Interestingly, although Aven appears evenly distributed in small vesicles within the cytosol, the protein was also localized to larger punctuate structures in approximately 3–5% of the cells (Figure 4, middle panels). Aven staining in these larger vesicular structures frequently overlapped with CathD staining (Figure 4, lower panels, see arrows). These results indicate that in MCF-7 cells, a fraction of Aven protein is co-localized in or at vesicular compartments with CathD, a prerequisite for physical interaction between Aven and its activating protease *in vivo*.

**Aven expression and proteolytic CathD activity are required to inhibit Caspase-3 activation in MCF-7/ Casp-3 cells.** To investigate the link between the CathD-mediated proteolysis of Aven and its ability to regulate apoptosis we first treated MCF7/Casp-3 cells (i.e., MCF-7 cells stably expressing transgenic Caspase-3<sup>30</sup>) with pepstatin A. As shown in Figure 5a, inhibition of CathD

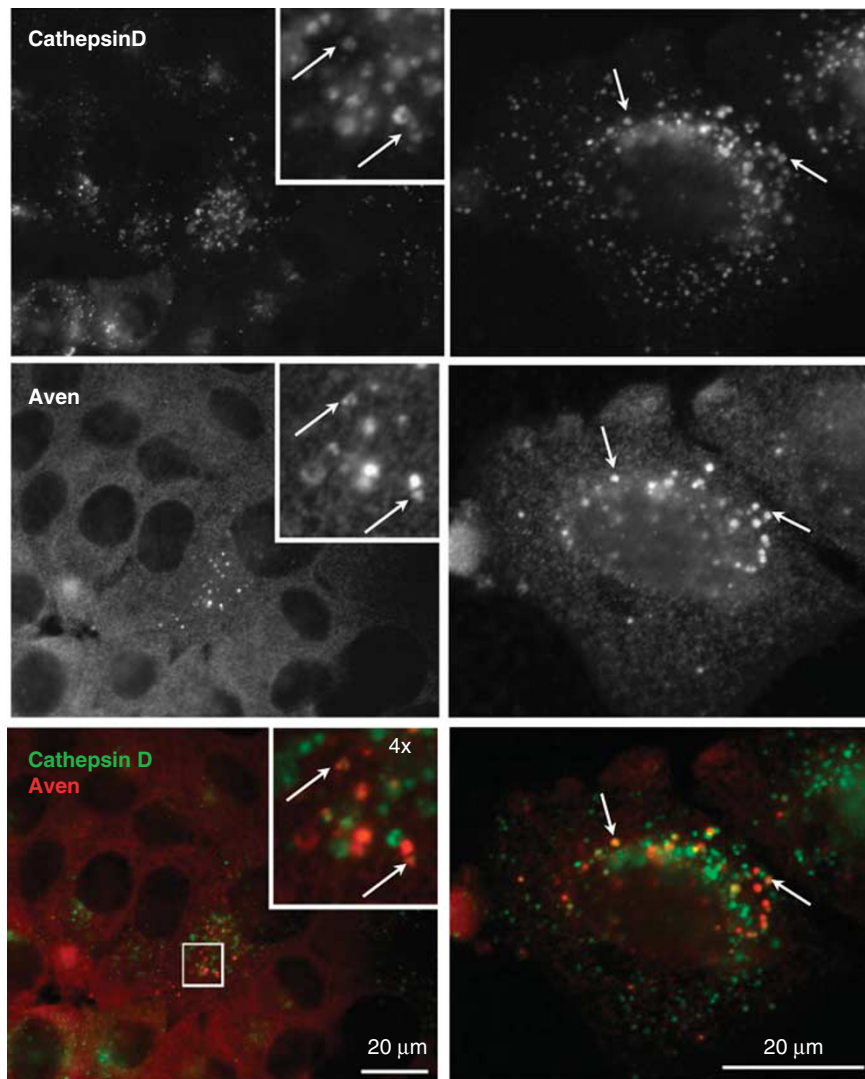


**Figure 4** Aven co-localizes with CathD in cytosolic vesicles. Immunofluorescence analysis was performed in fixed MCF-7 cells with goat anti-human CathD antibody and rabbit anti-human Aven B (recognizing aa 256–268), followed by detection with appropriate secondary antibodies. CathD shows staining in endosomal compartments (upper panels) whereas Aven displays a fine vesicular cytosolic staining pattern (middle panels). Some cells also display a larger punctuate Aven staining that overlaps with CathD signals (lower panels; Aven: red, CathD: green)

leads to increased Caspase-3 activation upon treatment of the cells with different apoptosis inducers. When *Aven* knockdown cells were treated with pepstatin A, no further increase in Caspase-3 activity was observed (data not shown), thereby emphasizing that Aven and CathD are regulating the same anti-apoptotic pathway.

A comparable increase in Caspase-3 activity as seen with pepstatin A-treated cells was observed when we abolished the expression of either Aven or CathD via stable shRNA transduction (Figure 5b). Interestingly, the levels of increased caspase activation were similar for both single knockdowns, again suggesting that these manipulations may affect the same pathway. Indeed, the simultaneous double knockdown of both *Aven* and *CathD* did not lead to additional increases in Caspase-3 activity as compared with both single knockdowns (data not shown).

**The inhibitory N-terminus is involved in Aven self-interactions.** Our results demonstrate that the N-terminal portion of Aven exerts an inhibitory influence on the anti-apoptotic function of the molecule (see Figure 1). We hypothesized that the regulation of Aven activity could be a result of either intra- or intermolecular Aven–Aven interactions mediated by the N-terminus. To test whether this protein region mediates self-interaction we performed co-immunoprecipitation experiments with various Flag-tagged Aven deletion constructs and a GFP-tagged version of the full-length Aven. As shown in Figure 6, full-length Aven-GFP protein efficiently co-precipitated with both the full-length Flag-Aven and the Flag-N-Aven 1–180 proteins, whereas the truncated Flag-ΔN-Aven 180–362 mutant lacking the N-terminus was unable to interact with Aven-GFP. Taken together, these experiments indicate that

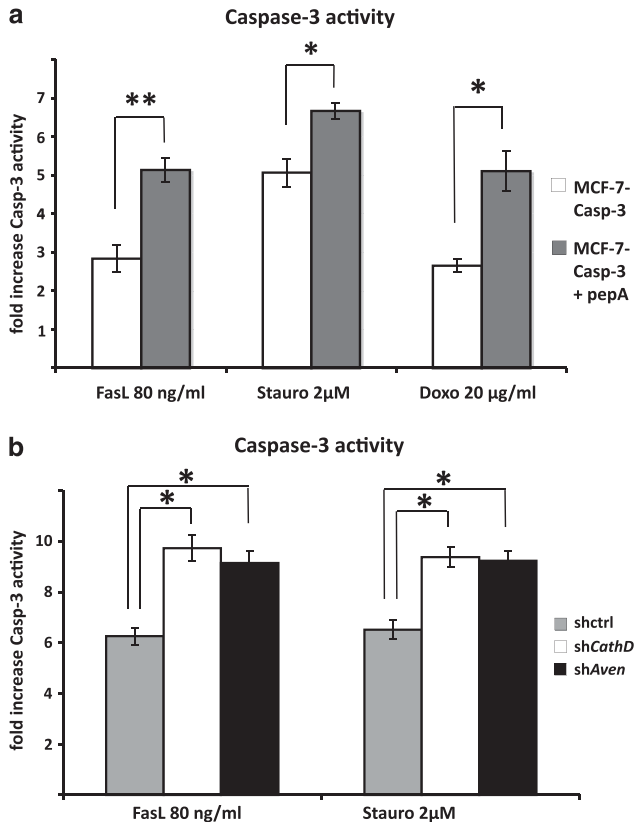


**Figure 5** Abrogation of CathD activity leads to increased Caspase-3 activity in MCF-7 cells after the induction of apoptosis. (a) Inhibition of CathD activity by treatment of MCF-7 cells with 40 µM pepstatin A leads to increased Caspase-3 activity after apoptosis induction by FasL, staurosporine or doxorubicin. Three independent experiments were performed, and the mean values are presented. Pepstatin A treatment resulted in significantly increased Caspase-3 activity following treatment with FasL, staurosporine or doxorubicin ( $P < 0.01$ ,  $P < 0.05$  and  $P < 0.05$ , respectively; Student's *t*-test). (b) The knockdown of either *Aven* or *CathD* in MCF-7 cells led to increased Caspase-3 activity after apoptosis induction by 80 ng/ml FasL or 2 µM staurosporine treatment. The experiment was repeated three times independently, and the mean values are shown. The treatment with both apoptosis inducers led to a significant increase in Caspase-3 activity in sh*Aven*- and sh*CathD*-transduced cells compared with control shRNA-transduced cells ( $P < 0.05$ , One-way ANOVA with LSD/Bonferroni *post-hoc* analysis). The bars in **a** and **b** represent standard errors, with \* and \*\* indicating  $P < 0.05$  and  $P < 0.01$ , respectively

Aven is capable of homomeric interactions, and the N-terminus of the protein is necessary for self-association.

## Discussion

Aven has been reported as an anti-apoptotic molecule that prevents apoptosome formation by directly binding to Apaf-1.<sup>13</sup> However, the mechanism by which the death-suppressing activity of this ubiquitously expressed protein is regulated remains unclear. In this study, we demonstrated the following: (i) the presence of an inhibitory N-terminal domain in Aven that downregulates its anti-apoptotic capacity; (ii) proteolytic removal of this inhibitory domain in intact cells, which can be abolished by either CathD downregulation or chemical inhibition; (iii) direct cleavage of the Aven N-terminus by CathD at positions aa 144/145 and aa 196/197 *in vitro*;

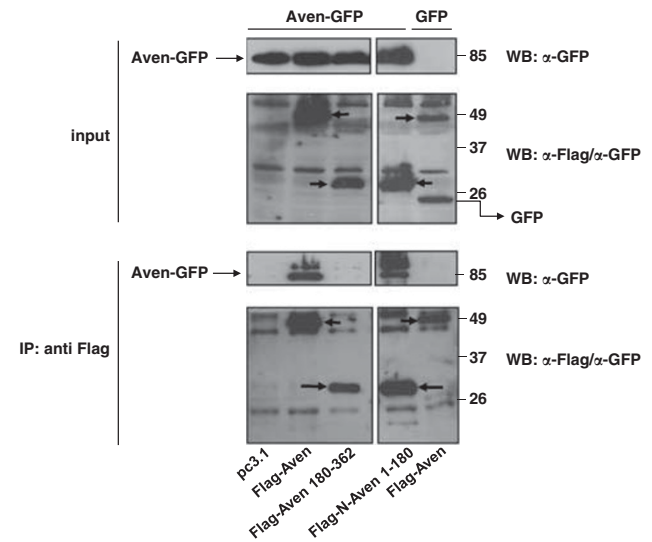


**Figure 6** Aven self-interacts via the N-terminus. HEK 293T cells were co-transfected with full-length *Aven-GFP*, various Flag-tagged *Aven* (deletion) constructs (full-length *Aven*,  $\Delta N$ -*Aven* 180–362, *N*-*Aven* 1–180) and empty vector (*pc3.1*). The transfection of *GFP* instead of *Aven-GFP* served as a negative control. Immunoprecipitation (IP) was performed using an anti-Flag antibody, and the membranes were probed with anti-Flag and anti-GFP antibodies. Input controls for each IP reaction are shown in the upper panel and represent 5% of total lysates. Arrows indicate the overexpressed Flag-tagged Aven mutants and the 25-kDa GFP band

(iv) partial co-localization of endogenous Aven and CathD in intact cells; and (v) N-terminus domain-dependent Aven self-association.

On the basis of our data, we propose a model of Aven activation by which its N-terminal inhibitory domain is removed by CathD-mediated cleavage, thereby unleashing Aven's cytoprotective activity. Our data establish that cleavage of Aven yielding the protective  $\Delta N$ -Aven fragment is CathD-dependent. Because we demonstrated the cleavage of purified Aven with the recombinant protease at positions aa 144/145 and aa 196/197 by mass spectrometry analysis (Figure 3), it is very likely that CathD directly hydrolyzes Aven, especially as this cleavage can be inhibited by the addition of pepstatin A. Both cleavage sites identified by mass spectrometry displayed processing events adjacent to Leu residues, which correlates with the specificity of CathD activity.<sup>31</sup> In general, cathepsins recognize stretches within their substrates rather than well-defined recognition sites (FI and KG, personal communication), and are therefore expected to cleave at multiple sites. The results obtained from the western blot analysis presented in Figure 2e (in particular the strength of the signal observed for the C-terminal Aven fragment detected with the anti-Aven CT antiserum that is similar in size to the Aven 180–362 polypeptide) indicate that aa position 196/197 is the primary CathD cleavage site, and that early trimming of the Aven protein by CathD might start at aa position 144/145. However, we cannot completely rule out the possibility that another protease (either directly or indirectly activated by CathD) is co-purified together with Aven from HEK 293T cells. The interaction between a protease and its substrate is in general very transient and difficult to detect.

Although CathD is one of the most abundant lysosomal proteases, several studies have also demonstrated the presence of active CathD outside the lysosomes. CathD is overexpressed and hyper-secreted by epithelial breast cancer cells where it promotes various cellular processes, including the degradation of basement membranes (for a review see Liaudet-Coopman *et al.*<sup>27</sup>). CathD also activates specific substrates in the pre-lysosomal endosome compartment (for a review see Garcia *et al.*<sup>29</sup>). In addition, large intracellular acidic vesicles found in both breast cancer cell lines and primary tumors contain phagocytosed extracellular material and high levels of CathD, which has the potential to degrade or activate important signaling molecules.<sup>32</sup>

Interestingly, a fine vesicular cytoplasmic staining pattern consistent with intracellular membrane localization has been reported for Aven, a finding that was supported by immunoblot analyses of fractionated cells.<sup>13</sup> Aven was associated primarily with the light-membrane fraction and was absent from the soluble S-100 fraction. These data are consistent with our immunofluorescence results that indicate that a portion of the Aven molecules is co-localizing with CathD in or at vesicular compartments (Figure 4).

Alternatively, Aven may also be cleaved by CathD in the cytoplasm. It has been reported that CathD is released from lysosomes into the cytosol at the early onset of apoptosis, thereby leading to the mitochondrial release of Cyt *c* and caspase activation (for a review see Masson *et al.*<sup>28</sup>). However, it can be envisaged that before activating the pro-death machinery, CathD must first activate anti-apoptotic proteins (e.g., Aven) in the cytosol to delay death and to allow for damage repair. In that regard, the overexpression of endogenous CathD typically observed in breast cancer cells<sup>28</sup> may lead to a constant release of CathD into the cytoplasm, thereby resulting in the activation of anti-death molecules such as Aven, and rendering tumor cells resistant to apoptosis. This notion is supported by the increased production of endogenous  $\Delta$ N-Aven observed in the breast cancer cell line MCF-7 (Figure 2b, left lane; endogenous  $\Delta$ N-Aven was also detected in longer exposures of Figure 2a blots, in empty vector-transfected cells (data not shown)).

The mechanism by which the N-terminal domain inhibits the anti-apoptotic activity of the Aven molecule remains to be elucidated. We found that the N-terminus can bind to full-length-Aven and that proteins lacking this domain lose their binding ability. It is possible that Aven self-association results in conformational changes or domain masking that interferes with the capacity of the full-length protein to inhibit apoptosis. In this scenario, the removal of the N-terminus by CathD would eliminate such inhibitory self-interactions and restore the full anti-apoptotic potential of Aven. The interaction of Aven with Bcl-x<sub>L</sub> is unlikely to provide insight into the capability of  $\Delta$ N-Aven to suppress cell death as Chau *et al.*<sup>13</sup> have already mapped the Bcl-x<sub>L</sub> binding site on the Aven molecule between aa 74 and 104. Therefore, in contrast to the full-length Aven protein, the anti-apoptotic  $\Delta$ N-Aven (lacking a larger N-terminal portion of Aven than the first 104 aa) is not able to bind to Bcl-x<sub>L</sub>, as we have demonstrated by co-immunoprecipitation (data not shown), thereby indicating that the molecular mechanism by which CathD cleavage of Aven protects cells against apoptosis is independent of Bcl-x<sub>L</sub>.

However, our data do not rule out the possibility that Aven may inhibit apoptosis by more than one molecular mechanism. Moreover, under certain conditions and/or cellular systems, full-length Aven may enhance the protective potential of Bcl-x<sub>L</sub>.<sup>14</sup> As far as the interaction of Aven with Apaf-1 is concerned, we could show by co-immunoprecipitation that  $\Delta$ N-Aven is still able to bind to Apaf-1, as is full-length Aven (data not shown). Although this interaction underlines the notion that Aven inhibits the mitochondrial apoptosis pathway, the protein may also exert other non-apoptotic cell-survival functions.

As the Aven N-terminus exhibits inhibitory characteristics it is interesting to note that mice express a shorter Aven transcript lacking most of the N-terminus (Acc. no. NM\_001165935.1). Both mRNA and protein expression levels of this murine Aven variant and its functional relevance have not been investigated.

Aven has also been reported to function in DNA damage repair and G<sub>2</sub>/M cell-cycle progression.<sup>33</sup> The addition of Aven mRNA coding for either the full-length or  $\Delta$ N72 human Aven protein (the latter lacking the N-terminal 72 aa) to cycling *Xenopus* egg extracts resulted in ATM kinase activation and the inhibition of mitotic entry. Similar effects were observed after the addition of purified recombinant His-tagged  $\Delta$ N72 Aven protein. It will be interesting to investigate whether the ATM-activating function of Aven also requires the removal of its N-terminus by CathD.

In essence, our results indicate that it is the proteolytic removal of Aven's N-terminus by CathD rather than the Aven expression level, which represents the major bottleneck in the generation of anti-apoptotic Aven activity. Therefore, Aven should be classified along with other proteins such as caspases and the Bcl-2 family member Bid (for a review see Ola *et al.*<sup>34</sup>), which require post-translational regulation by proteolytic processing to execute their apoptosis-regulating function.

## Material and Methods

**Cell culture, transfections and reagents.** The human colorectal carcinoma cell line RKO (ATCC CCL-2) and HEK 293T cells were cultured in Dulbecco's modified Eagle's medium (Gibco, Life Technologies, Darmstadt, Germany), while the human breast adenocarcinoma cell line MCF-7 (no Caspase-3 expression; ATCC HTB-22) and MCF-7/Casp-3 cells (MCF-7 cells stably transfected with *Caspase-3*) were cultured in 1640 Roswell Park Memorial Institute (RPMI) medium (Gibco). Both types of medium were supplemented with 10% fetal bovine serum (Sigma Aldrich, Munich, Germany), 4 mM L-glutamine (PAA Laboratories GmbH, Cölbe, Germany), penicillin and streptomycin (1 × from stock solution; PAA Laboratories GmbH). The cells were kept in an atmosphere of 5% CO<sub>2</sub> at 37 °C. MCF-7 and MCF-7/Casp-3 cells were kindly provided by R Jänicke (University of Düsseldorf, Germany).

RKO and MCF-7 cells were transfected with Lipofectamine (Invitrogen, Life Technologies, Darmstadt, Germany) and 293T cells were transfected with PEI (polyethylenimine, Sigma Aldrich) according to the manufacturers' instructions. Protease inhibitors pepstatin A (Sigma Aldrich), E-64 (Santa Cruz Biotechnology, Santa Cruz, CA, USA), z-VAD (Sigma), aprotinin and pAPMSF (both Santa Cruz Biotechnology) were dissolved in DMSO (Roth, Karlsruhe, Germany) and used at the concentrations indicated in the text.

**Expression constructs.** The following N-terminally Flag-tagged human Aven mutants were generated by PCR and cloned into *pcDNA3.1 (+) Zeo* (Invitrogen): full-length Aven (aa 1–362; kindly provided by M Rimpler (MDC Berlin, Germany)),  $\Delta$ N-Aven (aa 180–362) and N-Aven (aa 1–180). In addition, full-length Aven with a C-terminal 10 × His-tag was generated by PCR and cloned into the



*pcDNA3.1(+)* Zeo (*pcDNA3.1 flAven-10xHis*) vector. Full length *Aven* was cloned into a variant of the mammalian GFP expression vector *pEGFP-N1* (Clontech, Saint-Germain-en-Laye, France). *pEBB-HA-XIAP* was kindly provided by GM Cohen (MRC Toxicology Unit, University of Leicester, Leicester, UK), and *pcDNA3.1(+)* Zeo *His-Bcl-X<sub>L</sub>* was provided by R Eskes (Molecular Hematology, University Clinic Frankfurt, Frankfurt, Germany).

**shRNA constructs and lentiviral transduction.** The lentiviral *pLKO.1 puro* shRNA (Sigma) construct sequences for *Aven* and *CathD* downregulation are as follows:

*Aven* shRNA: 5'-CCGGGAGAATGATGAACAGGAAATCTCGAGATTTCCT GTTCATCTTCTTTTTG-3'; Control (scrambled) shRNA: 5'-CCGGCAACAAG ATGAAGAGACCAACTCGAGTTGGTGCTTTCATCTTGTGTTTTT-3'; *CathD* shRNA CD1: 5'-CCGGCATCACCTTCATCGCAGCCAACTCGAGTTGGCTGCGAT GAAGGTGATGTTTTT-3'; *CathD* shRNA CD2: 5'-CCGGACCTCGTTTGACATCCA CTATCTCGAGATAGTGGATGTCAAACGAGGTTTTTT-3'.

Lentiviral transduction was performed by transfection of  $1.5 \times 10^6$  HEK 293T cells per 10 cm dish with 2.5  $\mu$ g *pLKO.1 puro* shRNA vector, together with the packaging vectors *pMDG2* (1.625  $\mu$ g) and *8.91* (0.875  $\mu$ g) and polyethylenimine. Supernatants were harvested after 48 and 72 h and used directly for lentiviral transduction. MCF-7/Casp-3 cells were seeded ( $2 \times 10^5$  cells/well) in 6-well plates 1 day before transduction. Lentivirus-containing supernatants were mixed with 8  $\mu$ g/ml polybrene and added directly onto the cells. Cells were transduced during centrifugation at 1000 r.p.m. and 32 °C for 80 min and subsequently incubated at 37 °C/5% CO<sub>2</sub>. Supernatants were exchanged for fresh medium after 4–6 h, and the transduction was repeated on the next day. Cells were grown to confluence and subject to puromycin selection (2  $\mu$ g/ml) from the first passage onward.

**Antibodies.** The primary antibodies used are as follows: mouse monoclonal anti-Flag (M2, Sigma), rabbit polyclonal anti-Aven CT ( $\psi$ ProSci, raised against a 14-aa C-terminal peptide located in the region between aa 335 and aa 362 of the human *Aven* protein), mouse monoclonal anti-GFP (Stressgen Biotechnologies, Enzo Life Sciences, Lörrach, Germany), goat polyclonal anti-CathD (R&D Systems, Wiesbaden, Germany), anti-Ezrin (Invitrogen), anti-Aven A (aa 98–112) and anti-Aven-B (aa 256–268 (the latter two were a kind gift from JM Hardwick, John Hopkins University, Baltimore, MD, USA)). Fluorochrome-conjugated species-specific secondary antibodies for immunofluorescence were obtained from Jackson ImmunoResearch (West Grove, PA, USA). For immunoblot experiments, anti-mouse IgG, anti-rabbit IgG (Amersham Biosciences, GE Healthcare, Munich, Germany) and anti-mouse kappa light chain (Zymed, Life Technologies, Darmstadt, Germany) coupled to horseradish peroxidase were used as secondary anti-species antibodies.

**Apoptosis detection by flow cytometry.** RKO cells were transiently transfected with either control or *Aven* constructs and incubated overnight in the presence or absence of mitomycin C (Roche, Penzberg, Germany) at the indicated concentrations 24 h later. Alternatively, cells were treated for 16 h with 20 ng/ml soluble recombinant FasL (Alexis, Enzo Life Sciences, Lörrach, Germany), 1  $\mu$ g/ml anti-Flag M2 antibody (Sigma) for ligand crosslinking and 0.1  $\mu$ g/ml cycloheximide (Roche). For the quantification of apoptosis, cells were harvested at the appropriate time points, washed with phosphate-buffered saline (PBS) and fixed in ice-cold 70% ethanol before overnight incubation at 4 °C. Cells were then stained for 20 min with propidium iodide (50  $\mu$ g/ml) in 38 mM sodium citrate plus 10  $\mu$ g/ml RNase A at room temperature in the dark, and flow cytometry was performed using a FACScalibur (BD Biosciences, Heidelberg, Germany). Apoptotic cells with hypoploid DNA content were quantified in the 'subG1' region of the cell-cycle profile.

**Fluorimetric analysis of Caspase-3 activity.** For PEI-transfected HEK 293T cells, the *Casp-3/CPP32* Fluorimetric Assay Kit from BioVision (BioCAT GmbH, Heidelberg, Germany) was used according to the manufacturer's instructions. Briefly,  $5 \times 10^6$  cells were harvested and washed once with ice-cold 1  $\times$  PBS. After shock-freezing in liquid nitrogen, the pellets were stored at –80 °C. To assay for caspase activity, cell pellets were thawed on ice, re-suspended in 50  $\mu$ l of cell lysis buffer and incubated for an additional 10 min on ice. To induce apoptosome formation, lysates were incubated with 50  $\mu$ g/ml Cyt *c* (Sigma) and 1 mM dATP (Sigma) for 15 min at 37 °C. Next, 50  $\mu$ l of 2  $\times$  reaction buffer (containing 10 mM DTT) was added to each sample. After resuspending by pipetting (100  $\mu$ l end volume), the Caspase-3-specific substrate Ac-DEVD-AFC (*N*-acetyl-Asp-Glu-Val-Asp-7-amino-4-trifluoromethyl-coumarin) was added with a final

concentration of 30  $\mu$ M, and samples were transferred to a 96-well plate in triplicates (33  $\mu$ l in each well). Fluorescence was measured during 2 h of incubation at 37 °C using a fluorometer (FLUOstar OPTIMA, BMG Labtechnologies GmbH, Ortenberg, Germany).

For transduced MCF-7/Casp-3 cells, the fluorometric *Caspase-3* activity kit from Sigma Aldrich was used according to the manufacturer's instructions. Briefly,  $5 \times 10^4$  transduced cells were seeded in triplicates into clear-bottom 96-well plates ( $\mu$ clear, Greiner BioOne, Frickenhausen, Germany) and allowed to adhere for at least 6 h. Apoptosis was induced with FasL, staurosporine (Calbiochem, Merck, Darmstadt, Germany) or doxorubicin (Sigma; concentrations are indicated in the figure legends) over night. Plates were centrifuged with 1000 r.p.m. at room temperature for 5 min, and supernatants were then discarded. Lysis buffer (50  $\mu$ l) was added to each well, and lysis was performed at room temperature on a shaking platform (350 r.p.m.). Assay buffer (150  $\mu$ l) containing 17  $\mu$ M Caspase-3 fluorimetric substrate (Ac-DEVD-AFC) was added to each well, and fluorescence was measured during 2 h of incubation at 37 °C in a fluorometer (FLUOstar OPTIMA, BMG Labtechnologies GmbH).

**CathD cleavage of recombinant purified Aven-10xHis.** Two to four 14-cm dishes with  $3 \times 10^6$  HEK 293T cells were transfected with 20  $\mu$ g each of *pcDNA3.1 flAven-10xHis*. After 48 h, cells were harvested and incubated in 5 ml His-lysis buffer (50 mM Tris-HCl pH 7.5, 200 mM NaCl, 10 mM imidazole, 5% glycerol and 0.5% NP-40) for 30 min on ice before sonification (three 10 s pulses, strength 4, sonifier from Branson, Dietzenbach, Germany). Lysates were cleared by centrifugation at 14 000 r.p.m. and 4 °C for 10 min, and supernatants were added to 250  $\mu$ l Ni-NTA beads (Qiagen, Hilden, Germany) prewashed in His-lysis buffer. Binding was performed at 4 °C for 1–2 h. Supernatants were discarded and beads were washed three times with His-lysis buffer containing increasing concentrations of imidazole (20, 50 and 70 mM; Roth). Protein was eluted from the beads in a total volume of 200  $\mu$ l for 20 min at 4 °C using His-lysis buffer with 200 mM imidazole.

Purified *Aven* protein (2  $\mu$ g) was added to the CathD cleavage buffer (20 mM MES pH 6.5, 50 mM NaCl, 1 mM DTT) in a total volume of 20  $\mu$ l, and 0.3 units of human recombinant CathD (Calbiochem) were added to each reaction. Digestion was performed at 37 °C with constant shaking (300 r.p.m.), and samples were harvested by adding 5  $\times$  SDS-PAGE sample buffer and heating to 95 °C for 5 min at various time points. For the controls, one sample was incubated without CathD, and one sample was supplemented with 50  $\mu$ M pepstatin A before incubation. Samples were separated on 10% SDS-PAGE gels, blotted to nitrocellulose (Schleicher&Schuell, Dassel, Germany), and full-length and cleaved C-terminal *Aven* were detected with anti-His-tag-antibody.

**CathD digest of Aven-10xHis and mass spectrometry analysis.** To map the CathD cleavage sites of the *Aven* molecule, purified *Aven* protein (5  $\mu$ g) was diluted in 50  $\mu$ l of CathD cleavage buffer (50 mM MES, 50 mM sodium phosphate pH 7.4, 150 mM NaCl, 1 mM DTT, 1 mM EDTA; adjusted to pH 4.5 with 1N HCl). Recombinant human CathD (400 ng) was added to the protein mixture and samples were then incubated on a shaking platform at 100 r.p.m. for 10 or 30 min at 37 °C. The negative controls were incubated for 30 min either without the addition of CathD or with the addition of CathD and 10  $\mu$ M pepstatin A. After protease incubation, all samples were supplemented with 50 mM sodium phosphate pH 8.0 to a final volume of 500  $\mu$ l and solid guanidinium hydrochloride (2M final concentration). To label primary  $\alpha$ - and  $\epsilon$ -amines, 6.25  $\mu$ mol *N*-hydroxysuccinimide trideutero-acetate (NHS AcD<sub>3</sub>-acetate, synthesized in-house as previously described<sup>35</sup>) was added to each sample followed by a 2-h incubation at 30 °C. Each sample was then supplemented with 12.5  $\mu$ mol glycine and 37.5  $\mu$ mol hydroxylamine for a 20-min incubation at 30 °C to quench excess NHS AcD<sub>3</sub>-acetate and reverse possible O-acetylation, respectively. Proteins were then desalted on disposable NAP-5 columns (GE Healthcare Biosciences, Munich, Germany) and collected in 1 ml of 50 mM ammonium bicarbonate pH 8.0. Next, samples were boiled for 5 min, placed on ice for 5 min and digested overnight at 37 °C with 2  $\mu$ g trypsin (Promega Sequencing-Grade Modified Trypsin, Promega, Mannheim, Germany). Without pre-enrichment for N-terminal peptides, 100  $\mu$ l of each sample was acidified with 2  $\mu$ l formic acid and applied for LC-MS/MS analysis using a Thermo LTQ-Orbitrap XL mass spectrometer (2.5  $\mu$ l of sample was injected for each reading), which was operated as previously described.<sup>36</sup> Recorded MS/MS spectra data were examined using a locally installed version of the Mascot algorithm in the human subsection of the Swiss-Prot database. For this analysis, the following search parameters were used: the protease setting was set to semi-ArgC/P with up to two missed cleavages

allowed, fixed trideutero-acetate modification of lysine residues, variable acetate and trideutero-acetate modification of peptide N-termini, variable oxidation of methionine residues to methionine-sulfoxide, variable formation of pyroglutamate from N-terminal glutamine residues, precursor mass tolerance of 10 p.p.m. and fragment mass tolerance of 0.5 Da. Only the peptides that were ranked first and scored above the Mascot identity threshold at 95% confidence interval were withheld. Aven peptides that were trideutero-acetylated at the  $\alpha$ -amine were used to report CathD cleavage sites.

**Western blot analysis.** For immunoblotting assays, cells were washed in PBS and then lysed in lysis buffer (10 mM Tris-HCl (pH 7.5), 1.5 mM NaCl, 10 mM KCl, 10% SDS, 1 mM phenylmethylsulfonyl fluoride (PMSF; Sigma) and protease inhibitor cocktail (Roche)). Protein lysates (30–40  $\mu$ g) were separated by SDS-PAGE and transferred onto nitrocellulose membranes (Whatman, GE Healthcare, Munich, Germany). Equal loading was confirmed by Ponceau S (FLUKA BioChemika, Sigma Aldrich, Munich, Germany) staining of the membranes, or by incubation with antibodies recognizing housekeeping proteins. Subsequently, the membranes were blocked in 1  $\times$  TBS/3% non-fat milk (Applichem, Darmstadt, Germany) with 0.1% Tween 20 (Roti; blocking buffer) for 1 h and then incubated overnight at 4 °C with primary antibodies in blocking buffer. Dilutions of the respective antibodies are indicated in the figure legends. The membranes were washed three times with TBS/0.1% Tween 20 and incubated with peroxidase-conjugated secondary anti-species antibodies (anti-mouse/anti-rabbit 1 : 2000, anti-goat 1 : 5000) in blocking buffer for 1 h at room temperature. Protein bands were detected by chemiluminescence using the ECL Pico kit (Pierce Biosciences, Thermo Fisher Scientific, Bonn, Germany).

**Co-immunoprecipitation.** Transiently transfected HEK 293T cells (one 10-cm dish per immunoprecipitation (IP) were washed twice with 1  $\times$  PBS and lysed in 400  $\mu$ l lysis buffer (50 mM Tris-HCl (pH 7.5), 50 mM NaCl, 1 mM EGTA, 5% glycerol, 0.7% NP-40, proteinase inhibitor cocktail (Roche) per IP reaction. Lysis was performed on ice for 30 min and cellular debris was precipitated by centrifugation at 13 000 r.p.m. for 10 min at 4 °C. Ten percent of each reaction was removed for the input control. The remaining supernatants were pre-cleared once with pre-washed protein A/G agarose beads (Santa Cruz Biotechnology) at 4 °C for 1.5 h. Samples were then incubated at 4 °C overnight with 25–30  $\mu$ l fresh protein A/G agarose beads coupled to the mouse monoclonal anti-Flag antibody (Flag M2, Sigma). Captured protein complexes were washed three times in 400  $\mu$ l lysis buffer and eluted in 20–30  $\mu$ l of 1  $\times$  SDS-PAGE sample buffer for subsequent western blot analysis.

**Immunofluorescence analysis.** MCF-7 cells were fixed with 4% formaldehyde in PBS for 30 min at RT, washed twice with PBS, permeabilized with 0.2% saponin and labeled with primary and fluorochrome-conjugated secondary antibodies as described.<sup>37</sup> Cells were then analyzed on an Axiovert 200 M inverted fluorescence microscope equipped with an AxioCam CCD camera and AxioVision software (Zeiss, Göttingen, Germany).

**Statistics.** All experiments were performed at least three times to ensure reproducibility of the results. The data from apoptosis assays represent the mean of three to six independent experiments, and the Caspase-3 activity data illustrate the mean of three to eight independent experiments, each performed in triplicate. Error bars indicate the standard errors. Statistical analysis of two groups was done using the Student's *t*-test. Pairwise comparisons for experiments with more than two groups were performed by *post-hoc* analysis (LSD/Bonferroni or Games–Howell) after significant results were determined from one-way ANOVA testing.

#### Conflict of Interest

The authors declare no conflict of interest.

**Acknowledgements.** We thank R Jänicke (University of Düsseldorf, Germany), M Rimpler (MDC Berlin, Germany), GM Cohen (MRC Toxicology Unit, University of Leicester, UK), R Eskes (Molecular Hematology, University Clinic Frankfurt, Germany), and JM Hardwick (John Hopkins University, Baltimore, USA) for generously supplying the cells, expression constructs and antiserum (see Materials and Methods for details). FI is a Postdoctoral Fellow of the Research Foundation – Flanders (FWO-Vlaanderen). This work was supported by grants from

the German Cancer Aid Foundation (no. 108659; MZ) and the German National Genome Research Network (NGFN project N1KR-S12T23, MZ). Furthermore, the financial support by the Ministerium für Innovation, Wissenschaft und Forschung des Landes Nordrhein-Westfalen is gratefully acknowledged. KG acknowledges support from a research project of the FWO-Vlaanderen (G.0048.08).

- Brenner D, Mak TW. Mitochondrial cell death effectors. *Curr Opin Cell Biol* 2009; **21**: 871–877.
- Ow YP, Green DR, Hao Z, Mak TW. Cytochrome *c*: functions beyond respiration. *Nat Rev Mol Cell Biol* 2008; **9**: 532–542.
- Bao Q, Shi Y. Apoptosome: a platform for the activation of initiator caspases. *Cell Death Differ* 2007; **14**: 56–65.
- Li P, Nijhawan D, Budihardjo I, Srinivasula SM, Ahmad M, Alnemri ES *et al*. Cytochrome *c* and dATP-dependent formation of Apaf-1/caspase-9 complex initiates an apoptotic protease cascade. *Cell* 1997; **91**: 479–489.
- D'Amelio M, Tino E, Cecconi F. The apoptosome: emerging insights and new potential targets for drug design. *Pharm Res* 2008; **25**: 740–751.
- Hajra KM, Liu JR. Apoptosome dysfunction in human cancer. *Apoptosis* 2004; **9**: 691–704.
- Ledgerwood EC, Morison IM. Targeting the apoptosome for cancer therapy. *Clin Cancer Res* 2009; **15**: 420–424.
- Jiang X, Kim HE, Shu H, Zhao Y, Zhang H, Kofron J *et al*. Distinctive roles of PHAP proteins and prothymosin- $\alpha$  in a death regulatory pathway. *Science* 2003; **299**: 223–226.
- Qi X, Wang L, Du F. Novel small molecules relieve prothymosin  $\alpha$ -mediated inhibition of apoptosome formation by blocking its interaction with Apaf-1. *Biochemistry* 2010; **49**: 1923–1930.
- Beere HM, Wolf BB, Cain K, Mosser DD, Mahboubi A, Kuwana T *et al*. Heat-shock protein 70 inhibits apoptosis by preventing recruitment of procaspase-9 to the Apaf-1 apoptosome. *Nat Cell Biol* 2000; **2**: 469–475.
- Pandey P, Saleh A, Nakazawa A, Kumar S, Srinivasula SM, Kumar V *et al*. Negative regulation of cytochrome *c*-mediated oligomerization of Apaf-1 and activation of procaspase-9 by heat shock protein 90. *EMBO J* 2000; **19**: 4310–4322.
- Saleh A, Srinivasula SM, Balkir L, Robbins PD, Alnemri ES. Negative regulation of the Apaf-1 apoptosome by Hsp70. *Nat Cell Biol* 2000; **2**: 476–483.
- Chau BN, Cheng EH, Kerr DA, Hardwick JM. Aven, a novel inhibitor of caspase activation, binds Bcl-xL and Apaf-1. *Mol Cell* 2000; **6**: 31–40.
- Kutuk O, Temel SG, Tolunay S, Basaga H. Aven blocks DNA damage-induced apoptosis by stabilising Bcl-xL. *Eur J Cancer* 2010; **46**: 2494–2505.
- Choi J, Hwang YK, Sung KW, Kim DH, Yoo KH, Jung HL *et al*. Aven overexpression: association with poor prognosis in childhood acute lymphoblastic leukemia. *Leuk Res* 2006; **30**: 1019–1025.
- Paydas S, Tanriverdi K, Yavuz S, Disel U, Sahin B, Burgut R. Survivin and aven: two distinct antiapoptotic signals in acute leukemias. *Ann Oncol* 2003; **14**: 1045–1050.
- Breznecanu ML, Volp K, Bosser S, Solbach C, Lichter P, Joos S *et al*. HMGB1 inhibits cell death in yeast and mammalian cells and is abundantly expressed in human breast carcinoma. *FASEB J* 2003; **17**: 1295–1297.
- Rabenhorst U, Beinoraviciute-Kellner R, Breznecanu ML, Joos S, Devens F, Lichter P *et al*. Overexpression of the far upstream element binding protein 1 in hepatocellular carcinoma is required for tumor growth. *Hepatology* 2009; **50**: 1121–1129.
- Scaffidi C, Schmitz I, Zhu J, Korsmeyer SJ, Krammer PH, Peter ME. Differential modulation of apoptosis sensitivity in CD95 type I and type II cells. *J Biol Chem* 1999; **274**: 22532–22538.
- Massard C, Zermati Y, Pauleau AL, Larochette N, Metivier D, Sabatier L *et al*. hTERT: a novel endogenous inhibitor of the mitochondrial cell death pathway. *Oncogene* 2006; **25**: 4505–4514.
- Seong GJ, Park C, Kim CY, Hong YJ, So HS, Kim SD *et al*. Mitomycin-C induces the apoptosis of human Tenon's capsule fibroblast by activation of c-Jun N-terminal kinase 1 and caspase-3 protease. *Invest Ophthalmol Vis Sci* 2005; **46**: 3545–3552.
- Gour-Salin BJ, Lachance P, Magny MC, Plouffe C, Menard R, Storer AC. E64 [trans-epoxysuccinyl-L-leucylamido-(4-guanidino)butane] analogues as inhibitors of cysteine proteinases: investigation of S2 subsite interactions. *Biochem J* 1994; **299** (Part 2): 389–392.
- Vandenabeele P, Vanden Berghe T, Festjens N. Caspase inhibitors promote alternative cell death pathways. *Sci STKE* 2006; **2006**: pe44.
- Levy JH, Sypniewski E. Aprotinin: a pharmacologic overview. *Orthopedics* 2004; **27** (6 Suppl): s653–s658.
- Laura R, Robison DJ, Bing DH. (p-Amidinophenyl)methanesulfonyl fluoride, an irreversible inhibitor of serine proteases. *Biochemistry* 1980; **19**: 4859–4864.
- Umezawa H, Aoyagi T, Morishima H, Matsuzaki M, Hamada M. Pepstatin, a new pepsin inhibitor produced by Actinomycetes. *J Antibiot (Tokyo)* 1970; **23**: 259–262.
- Liaudet-Coopman E, Beaujourn M, Derocq D, Garcia M, Glondu-Lassis M, Laurent-Matha V *et al*. Cathepsin D: newly discovered functions of a long-standing aspartic protease in cancer and apoptosis. *Cancer Lett* 2006; **237**: 167–179.
- Masson O, Bach AS, Derocq D, Prebois C, Laurent-Matha V, Pattingre S *et al*. Pathophysiological functions of cathepsin D: targeting its catalytic activity versus its protein binding activity? *Biochimie* 2010; **92**: 1635–1643.

29. Garcia M, Platet N, Liaudet E, Laurent V, Derocq D, Brouillet JP *et al*. Biological and clinical significance of cathepsin D in breast cancer metastasis. *Stem Cells* 1996; **14**: 642–650.
30. Janicke RU, Sprengart ML, Wati MR, Porter AG. Caspase-3 is required for DNA fragmentation and morphological changes associated with apoptosis. *J Biol Chem* 1998; **273**: 9357–9360.
31. Impens F, Colaert N, Helsens K, Ghesquiere B, Timmerman E, De Bock PJ *et al*. A quantitative proteomics design for systematic identification of protease cleavage events. *Mol Cell Proteomics* 2010; **9**: 2327–2333.
32. Montcourrier P, Mangeat PH, Salazar G, Morisset M, Sahuquet A, Rochefort H. Cathepsin D in breast cancer cells can digest extracellular matrix in large acidic vesicles. *Cancer Res* 1990; **50**: 6045–6054.
33. Guo JY, Yamada A, Kajino T, Wu JQ, Tang W, Freel CD *et al*. Aven-dependent activation of ATM following DNA damage. *Curr Biol* 2008; **18**: 933–942.
34. Ola MS, Nawaz M, Ahsan H. Role of Bcl-2 family proteins and caspases in the regulation of apoptosis. *Mol Cell Biochem* 2011; **351**: 41–58.
35. Staes A, Impens F, Van Damme P, Rutten B, Goethals M, Demol H *et al*. Selecting protein N-terminal peptides by combined fractional diagonal chromatography. *Nat Protoc* 2011; **6**: 1130–1141.
36. Ghesquiere B, Colaert N, Helsens K, Dejager L, Vanhaute C, Verleysen K *et al*. *In vitro* and *in vivo* protein-bound tyrosine nitration characterized by diagonal chromatography. *Mol Cell Proteomics* 2009; **8**: 2642–2652.
37. Theos AC, Berson JF, Theos SC, Herman KE, Harper DC, Tenza D *et al*. Dual loss of ER export and endocytic signals with altered melanosome morphology in the silver mutation of Pmel17. *Mol Biol Cell* 2006; **17**: 3598–3612.

Supplementary Information accompanies the paper on Cell Death and Differentiation website (<http://www.nature.com/cdd>)